

REVIEW

View Article Online

View Journal | View Issue



Cite this: *Inorg. Chem. Front.*, 2023, **10**, 7126

The role of niobium in layered oxide cathodes for conventional lithium-ion and solid-state batteries

Barbara Nascimento Nunes,  *^a Wessel van den Bergh, *^a Florian Strauss, ^a Aleksandr Kondrakov, ^{a,b} Jürgen Janek  ^{a,c} and Torsten Brezesinski  *^a

Layered transition metal oxides (LTMOs), such as the $\text{LiNi}_x\text{Co}_y\text{Mn}_{1-x-y}\text{O}_2$ family, are the primary class of cathode active materials (CAMs) commercialized and studied for conventional lithium-ion (LIB) and solid-state battery (SSB) application. Despite nearly three decades of progress in improving stability, capacity, and cost, research has intensified to match global demand for high-performance materials. Nevertheless, (de)lithiation leads to irreversible degradation and subsequent capacity fading due to (chemo)mechanical particle disintegration and (electro)chemical side reactions. In this regard, surface and bulk modifications of CAMs by coating and doping/substitution are common strategies to enhance and support the electrochemical performance. Niobium has been featured in many studies exhibiting its advantages as a bulk dopant, where its ionic radius and unique valence character with respect to the metals used in LTMOs help prevent different degradation phenomena and therefore enhance performance. In addition, several niobium-based oxides (LiNbO_3 , Li_3NbO_4 , Nb_2O_5 , etc.) have been employed as a coating to increase cycling stability and rate capability through reduced surface degradation. Herein we illustrate how niobium serves as a coating constituent and a dopant, and discuss current understanding of underlying mechanisms, gaps in knowledge, and considerations for its use in a coating and/or as dopant in LTMO cathodes.

Received 14th September 2023,
Accepted 7th November 2023

DOI: 10.1039/d3qi01857a

rs.c.li/frontiers-inorganic

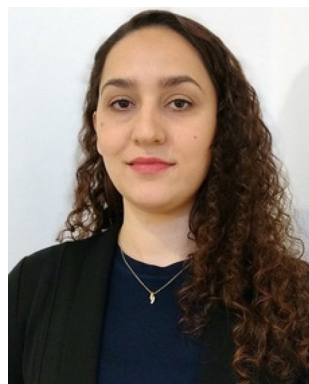
^aBattery and Electrochemistry Laboratory (BELLA), Institute of Nanotechnology, Karlsruhe Institute of Technology (KIT), Hermann-von-Helmholtz-Platz 1, 76344 Eggenstein-Leopoldshafen, Germany. E-mail: barbara.nunes@kit.edu, wessel.saarberg@kit.edu, torsten.brezesinski@kit.edu

^bBASF SE, Carl-Bosch-Str. 38, 67056 Ludwigshafen, Germany

^cInstitute of Physical Chemistry & Center for Materials Research (ZfM/LaMa), Justus-Liebig-University Giessen, Heinrich-Buff-Ring 17, 35392 Giessen, Germany

1. Introduction

The combination of higher energy density, cycle life, safety, and faster charging, compared to other battery chemistries, has promoted lithium-ion batteries (LIBs) to a widespread power source for a broad range of applications, from portable electronic devices to electric vehicles and stationary energy-storage systems.¹ Since LiCoO_2 (LCO) came about as a new cathode active material (CAM) for high energy density batteries



Barbara Nascimento Nunes

Barbara Nascimento Nunes has a chemistry background and completed her cotutelle PhD in 2022, jointly from Leibniz University Hannover and Federal University of Uberlandia. Currently, she is a post-doctoral researcher at BELLA at the Karlsruhe Institute of Technology focusing on the development of cathode materials for lithium-ion batteries.



Wessel van den Bergh

Wessel van den Bergh is a post-doctoral researcher at BELLA at the Karlsruhe Institute of Technology. His research interests are focused on the use of controlled design methodologies to study the relationship between material features and electrochemical behavior for energy-storage applications.



and subsequently the commercialization of LIBs in 1991,^{2,3} alternative layered oxides have been explored to improve battery performance and reduce the dependence on cobalt, which has high ethical and economic costs.⁴⁻⁷ For instance, LiNiO₂ (LNO) represents a promising alternative with a local maximum in theoretical specific capacity, however its poor structural stability and low reversible cycling performance limit current commercialization.⁸ Other materials, namely the LiNi_xCo_yMn_{1-x-y}O₂ (NCM or NMC) and LiNi_xCo_yAl_{1-x-y}O₂ (NCA) families, do allow for better cycling stability with the sacrifice of capacity. NCMs have become one of the main classes of CAMs commercialized and studied for LIBs and solid-state batteries (SSBs).^{9,10} Due to the global demand for improved batteries in all aspects, there is a general movement to higher nickel content for greater capacity, a transition from flammable liquid electrolyte to solid-electrolyte-based lithium batteries, and evermore material modifications to improve both surface and bulk properties of CAM. Each of these movements in research manifests new challenges, mostly including the need to reduce material degradation and kinetic limitations.

Electrochemical, mechanical, and chemical changes contribute to issues of limited kinetics and stability observed in layered transition metal oxides (LTMOS). Mechanical degradation originates from repeated volume changes in the CAM associated with phase transitions during (de)lithiation that leads to the disintegration of cathode particles and oxygen release from the lattice. This oxygen partially undergoes follow-up reactions with the electrolyte forming CO₂ among other undesired species.^{11,12} The most common solution is inclusion of dopants, which can suppress the most mechanically demanding phase transitions (H2 → H3),¹³ or protective surface coatings minimizing gas evolution, for example.^{14,15} Chemically, the presence of HF in the commercially common LiPF₆-based liquid electrolyte due to trace water results in dissolution of TM species. Here, sacrificial compounds or coatings are introduced to NCM cathodes as a strategy for mitigating this issue. As an electrochemical degradation mechanism, there is the decomposition of electrolyte, leading to the formation of a resistive surface layer (cathode electrolyte inter-

phase, CEI), as well as the phenomenon of degradation of bulk NCM layered structure.^{16,17} To address these concerns, specific solutions involving coatings and dopants are implemented in the quest to develop improved battery materials. Coatings, which serve as a controlled, stable CEI, ideally need to offer high ionic conductivity, good chemical resistance, and a simple synthesis process.^{18,19} With respect to doping strategies, dopants can modify either a portion of the subsurface or the entirety of the bulk. Regardless of the depth of incorporation, a dopant ideally serves to stabilize the structure of the CAM, such as forming stronger metal–oxygen (M–O) bonds, to reduce oxygen release or increase lithium diffusivity.

Selection of elements and/or compounds to serve as dopants and/or coatings is an on-going process, where the untrained eye may feel that the field is collectively sifting through the periodic table. Regardless of the breadth of exploration for the next best coating or dopant, there have been reports of promising candidates for mainstream implementation. Niobium has been featured in many studies exhibiting its advantages as an elemental dopant and of its various oxide phases (LiNbO₃, Li₃NbO₄, Nb₂O₅, etc.) as coating agents. Overall, its common and most stable oxidation state of Nb⁵⁺ shows high affinity to oxygen and forms thermally and chemically stable oxides.²⁰ In addition, it has a comparable ionic radius of 0.64 Å, yet distinct valence character, with respect to the common metal species used in LTMOS, e.g., Ni³⁺ (0.56 Å), Ni²⁺ (0.69 Å), Co³⁺ (0.55 Å), Mn³⁺ (0.58 Å), Al³⁺ (0.54 Å), and Li⁺ (0.76 Å).²¹ These characteristics translate to an observed reduction in degradation and improvements to lithium diffusion kinetics when Nb⁵⁺ is employed as a dopant. Other element dopants with comparable ionic radius and higher valence than the TMs in LTMOS, such as V⁵⁺,²²⁻²⁴ Ta⁵⁺,²⁵⁻²⁷ Mo⁶⁺,²⁸⁻³⁰ and W⁶⁺,³¹⁻³³ have also been reported to exhibit similar improvements. Another work has outlined the impact of these and various other dopants and coating materials on Ni-rich CAMs.³⁴ Experimentally, many niobium precursors are reported in the literature for use in both doping and coating approaches. A crucial point to consider is that the specific niobium location in lithium-based LTMOS depends on



Florian Strauss

Florian Strauss received his PhD in 2016, under the supervision of Prof. Tarascon (Collège de France, Paris) and Prof. Dominko (National Institute of Chemistry, Ljubljana). He spent several years as a post-doctoral researcher at BELLA at the Karlsruhe Institute of Technology and is currently a junior group leader at the Institute of Nanotechnology exploring novel electrolytes for solid-state batteries.



Aleksandr Kondrakov

Aleksandr Kondrakov received his diploma in Chemistry from the Lomonosov Moscow State University in 2010 and a PhD in Chemistry from the Karlsruhe Institute of Technology in 2014. After postdoctoral years spent at BELLA, he joined BASF Battery Materials in 2017 working on the development of layered Ni-rich oxide cathode materials. As a lab team leader of BELLA, he focuses on the research of next-generation battery materials.



which benefit the performance and stability of the CAM. First, coatings serve as a physical barrier between CAM and electrolyte, which mitigates the formation of (excess) CEI as well as side reactions, such as metal dissolution, electrolyte consumption, and gas formation. Second, designed coatings ideally have a greater permittivity (1/resistance) than “native” CEIs, thereby minimizing the overpotential that may otherwise intensify side reactions and lead to reduced capacity. Similar benefits are observed in SSBs, where (electro)chemical solid electrolyte decomposition and related performance decay are prevented.^{51,52} Lastly, experimental data suggest that coatings can increase the temperature at which cathodes experience thermal runaway, which is critical for commercial liquid-electrolyte-based LIBs.^{35,53–56}

Despite a plethora of compositional options for coatings, Nb-based ones represent a promising method to stabilize cathode/electrolyte interfaces. LiNbO_3 can be considered the quintessential Nb-based coating and can be prepared in multiple ways, including sol-gel,^{42,53,57–73} dry coating,^{55,61,74–79} and atomic layer deposition (ALD).^{80,81} Sol-gel derived coatings require the least demand with regards to equipment, and the procedure is mature. Typically, CAM particles are suspended in a solvent together with Nb-alkoxides or chlorides and an extra source of lithium (usually lithium ethoxide) is included. This process can take place in alcohols, which are subsequently evaporated to yield a gel. *Via* changing the precursor ratios and adding a lithium source, different Nb-oxide-based compositions, such as Nb_2O_5 , LiNbO_3 , and Li_3NbO_4 , can be targeted. This mixture is then calcined (usually in air or oxygen) at different temperatures, which determines whether niobium remains at the surface or migrates into the bulk of the CAM.⁵⁶ However, sol-gel derived coatings are observed to suffer from non-uniformity, although they can be rapidly prepared through a simple process. Moreover, it has been recently recognized that coatings prepared *via* the sol-gel method always contain (amorphous) lithium carbonate, which appears to have a significant impact on the resulting performance of the CAM, especially in SSBs.^{67,73,82–84} Dry coating is an alternative procedure, where preformed (preferably nanocrystalline) LiNbO_3 is mixed with CAM powder under moderate or high energy conditions (milling). The mixture is then calcined to sinter the coating and the CAM together. While requiring specialized yet simple equipment, the use of cheaper starting materials is attractive, even if coating uniformity is still non-ideal. To yield a conformal coating on CAM particles, ALD is the method of choice, however at the expense of costly equipment.

Regardless of the technique, Nb-based oxides exhibit stability against aggressive acid conditions. For instance, a clear illustration of this resilience is observed on sample preparation protocols for inductively coupled plasma (ICP) optical emission spectroscopy (OES), where concentrated acids at high temperatures are required to achieve niobium dissolution.^{85,86} It should be noted that alternatively employing a protective coating as a sacrificial HF scavenger might not be an optimal design choice. Furthermore, scavengers with extensive surface areas (nanoparticles) can be introduced as additives rather

than implementing a more complex coating process. Regardless, it is clear that Nb-based coatings do reduce metal dissolution, where they most likely act as a physical barrier preventing TM ion migration to the electrolyte.⁷⁶

To understand composition–morphology related properties of nanoscale coatings, a thorough characterization down to the atomic scale is needed. Initially, scanning electron microscopy (SEM) is often performed to confirm that the particle morphology is not affected during the coating formation. For instance, Fig. 1a–f shows images of Nb_2O_5 -coated NCM622 in comparison to the pristine material, where the presence of Nb_2O_5 did not alter the overall morphology or average particle size of CAM.⁷⁶ While there may be slight textural differences at the surface,^{70,72} additional analytical techniques are needed to characterize the morphology and composition of the coating. Coatings prepared *via* sol-gel methods tend to show a partial agglomeration on the CAM surface.^{70,72} It should be noted that several studies explicitly mention the thickness. The optimal thickness can generally vary within the range of ~2 to 10 nm.^{42,56,58,60,62,65,67,68,79–81,87–89} Nevertheless, only one of them quantifies the degree of uniformity or variation in thickness. This particular study employed atomic force microscopy (AFM) to measure particle roughness, which decreased with added coating, likely suggesting a reduction in initial porosity.⁸¹ This is in the context of reports that vary coating thickness by molar or weight percentage and observe differences in performance. In general, both extremely thin and thick coatings come with limitations. Very thin coatings fail to fully cover particles, while thick coatings hinder charge transfer, sacrificing rate capability and reducing specific capacity due to increased resistance.^{58,80,87,88} Therefore, considering that physical thickness of the coating rather than molar or weight fraction with respect to the CAM will dictate performance, we recommend examining thickness as being more relevant. To do so, thin sample specimens prepared by focused ion beam (FIB) milling/slicing are required. This allows for an examination of the



Fig. 1 (a–c) SEM images of a pristine $\text{LiNi}_{0.6}\text{Co}_{0.2}\text{Mn}_{0.2}\text{O}_2$ (NCM622) sample. (d–f) SEM images of coated NCM622 prepared from a ball-milling method with Nb_2O_5 (0.5 mol%). Reproduced with permission from ref. 76. Copyright 2021, Elsevier.



coating *via* energy dispersive X-ray spectroscopy (EDS) line scans^{64,87} (see Fig. 2a and b) and transmission electron microscopy (TEM),^{64,80,87} which is however spatially limited to a small range of the surface layer. Interestingly, X-ray photoelectron spectroscopy (XPS) analysis reveals that the distribution of coating ions can strongly depend upon the choice of coating method. XP spectra were obtained by gradually removing surface layers through ion etching.⁸⁷ A thicker layer formed when using a coating methodology of introducing niobium, while including niobium with the precursor reagents before CAM synthesis led to ion migration into the bulk structure.

Additionally, due to the proclivity of niobium to diffuse into the bulk lattice, it stands out that few works examined the gradient of niobium concentration from the surface to the core.^{35,60,65,87,90} With the advent of studies beginning to understand the implications of gradient-doped NCM CAMs, this is a feature that should be studied in detail when observed. X-ray diffraction (XRD) analysis serves to see the effect of niobium in the bulk, whose introduction usually affects the lattice parameters.⁷⁹ The effect of niobium as a bulk dopant is discussed in the doping section below. XRD also shows evidence that procedures that originally target Nb₂O₅ coatings may convert it to LiNbO₃,^{77,79} even in the absence of an additional lithium source.⁵⁶ One can verify the formation of a specific coating with X-ray absorption spectroscopy (XAS), even when the coating is below the limit of detection for XRD. Fig. 3 displays peaks associated with transitions from the 2p orbital of niobium in different reference materials. In this particular case, peak shift analysis provided insight into the chemical state of the coating.⁵⁷ In the absence of a deliberate external source, it is probable that residual lithium on the CAM's surface or lithium from within the bulk serves as the source for LiNbO₃ formation. This may lead to the unintended



Fig. 3 XAS of the Nb L₃-edge of reference materials with Nb⁵⁺ oxidation state. Dotted lines C and D correspond to LiNbO₃ peak position, while dotted line E is peak position of each reference material. Reproduced with permission from ref. 57. Copyright 2023, American Chemical Society.

increase of Li⁺/Ni²⁺ cation mixing (antisite defects, Ni_{Li}[•]) that degrades the performance of the CAM, as discussed below.

Crystalline LiNbO₃ can be detected through XRD analysis. However, employing XRD for characterizing nanoscale coatings is often impractical due to the limited sensitivity of most in-house instruments.^{87,91,92} Any observation of reflections from coatings likely comes from agglomerated species or coatings that exceed practical thickness, as shown in Fig. 4, in which at 20 wt% loading, agglomeration and layering is large

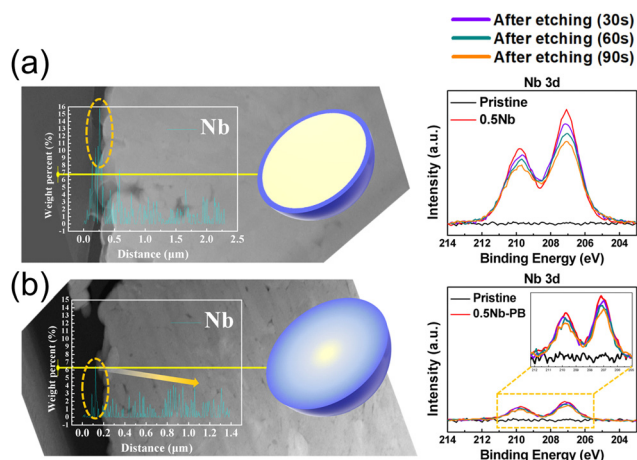


Fig. 2 Cross-sectional scanning TEM (STEM) with EDS line profiles of Nb across the yellow line for LiNi_{0.82}Co_{0.12}Mn_{0.06}O₂. Shown to the right is the corresponding material's Nb 3d XPS spectra with different etch times. Panel (a) refers to a coating methodology of introducing Nb, while panel (b) refers to a route of including Nb with the precursor reagents. Adapted from ref. 87. Copyright 2021, American Chemical Society.

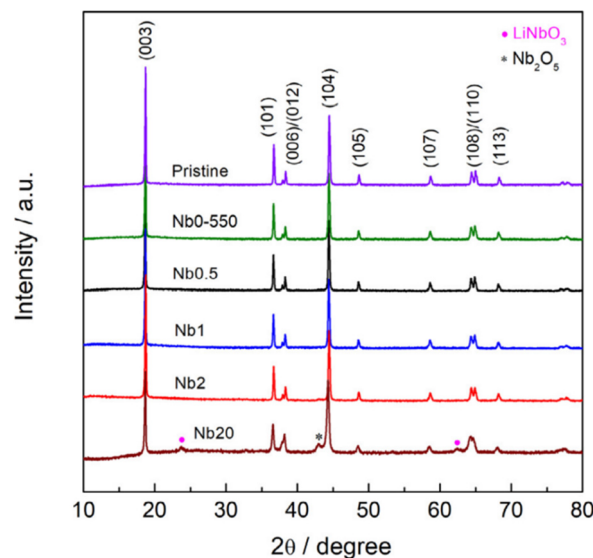


Fig. 4 XRD patterns of NCM622 coated with different loadings (wt%) of LiNbO₃ prepared from an ammonium niobium oxalate sol-gel method. Reproduced with permission from ref. 56. Copyright 2021, Elsevier.



enough to show Nb-based reflections.^{56,58,75} XRD signals linked to the coating are evident in several sol-gel-based approaches^{56,58,59,70,93} in contrast to ALD-based reports.⁸⁷

XPS is commonly used to characterize the composition and state of the LTMO surface, however, frequently, extrapolations are made that require careful consideration. Firstly, XPS (Nb 3d) can detect the oxidation state of the niobium,^{53,56,94} which is usually observed to be +5 and can reflect either LiNbO₃ or Nb₂O₅. This can be applied to other atomic species; works reporting Nb₂O₅ coatings performed XPS (Ni 2p) to note an increase in Ni²⁺ species at the surface,^{76,79} likely due to the LiNbO₃ formation (resulting in extraction of lithium from the bulk of the CAM). Simultaneously, some ions diffuse into the bulk, and the high valence state of niobium lowers the nickel oxidation state to Ni²⁺, thereby driving it into the lithium layer.^{60,77} LiNbO₃ does not affect the Ni²⁺ fraction at milder temperatures (*e.g.*, ≤550 °C).^{42,69} In contrast to these observations, other work describes that niobium coating actually reduces near-surface Ni²⁺,⁷⁸ which could also be expected for a surface-stabilizing coating. The authors also show XRD Rietveld refinements of their LTMO and coated material, indicating a lower fraction of Ni_{Li} defects, however often do so with suspiciously low *R*_{wp} values for lab-scale diffractometers.^{64,95} As will be discussed later, complementary techniques to determine the effect of niobium on point defects should be employed to build a stronger case. Secondly, XPS can indicate the migration of niobium from the surface to the bulk through loss of intensity of the corresponding spectra, which correlates with increasing preparation temperature.³⁵ When looking at other XPS peaks, it is observed that Nb-based coatings reduce the fraction of Li₂CO₃,³⁵ a surface carbonate that relates to decomposed electrolyte,⁵⁵ air exposure,^{83,96} and insulating LiF. Degradation of the surface can be observed with XPS⁵⁸ and can be correlated with electrochemical measurements of average surface resistance, charge-transfer resistance, and their rate of growth in LIBs and SSBs.⁹³

Turning to performance itself, a meta-analysis of both LIBs and SSBs with LiNbO₃-coated NCM CAMs reveals generalizable

trends and indicators of its true utility. Fig. 5 is a box-and-whisker plot of a meta-analysis of coated NCMs. Comparisons of relative performance changes were made between the self-described best coating reported and their baseline NCM material; a method that removes the case-by-case comparison and the many minor differences in methodology and testing. Furthermore, unless otherwise demonstrated in the work with certainty, all coatings are assumed to be LiNbO₃, despite claims of Nb₂O₅, due to their lack of support evidence to the case. Lastly as a note, due to the variation in number of cycles reported across works, a standard of 100 cycles was selected. For cases, where this information was not explicitly provided, an estimate was calculated based on reported cycling stability and assuming a linear trend of degradation for all materials. This estimation methodology is the case for both the data presented for coatings as well as dopants shown in a later section. Starting with LIB samples, Fig. 5 shows that the introduction of LiNbO₃ as a coating had an insignificant effect on the initial discharge capacity (median = 3.3%) while being able to significantly improve cycle retention (median = 12%) and capacity at 1C rate (median = 8.0%). This likely reflects the reduction in surface decomposition and therefore reduced resistance of the material. Regarding SSBs, there is an increase in all metrics, first-cycle capacity (median = 18%), cycle stability (median = 10%), and capacity at 1C rate (median = 28%). While not surprising that there are improvements, it is important to note that the relative increases in rate capability and first-cycle capacity are greater for SSBs than LIBs. This is most likely due to the formation of a much more insulating interface (decomposition) layer in SSBs when using uncoated CAM as compared to LIBs. Regardless of the electrolyte, ionic conductivity of amorphous LiNbO₃ is significantly higher than of base NCM. This reflects an average observed relative increase in diffusivity of LiNbO₃-coated NCMs by 120% ± 150% (mean ± std. dev., *n* = 6) and 74% ± 53% (mean ± std. dev., *n* = 3) for LIBs and SSBs, respectively.^{42,56,58,74,76,77,79,81,87,97}

Despite being a point parroted in introductions as critical to improving LIBs, thermal stability, *i.e.*, onset temperature of

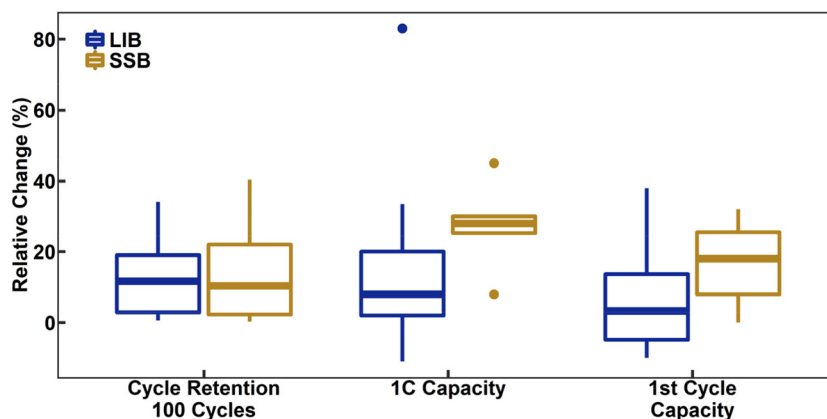


Fig. 5 Box-and-whisker plot of the relative change of capacity retention after 100 cycles, 1C capacity, and first-cycle capacity of LiNbO₃ coatings with respect to "bare" NCM CAMs for both LIB and SSB systems. For cycle retention, *n* = 19 and 9 for LIB and SSB, respectively. For 1C capacity, *n* = 17 and 6 for LIB and SSB, respectively. For first-cycle capacity, *n* = 18 and 11 for LIB and SSB, respectively.



Table 2 Summary of main electrochemical performances from the literature of Nb-doped LTMOs for LIBs, their respective base material, as well as Nb source and its amount (SC = single crystal, DC = specific discharge capacity, CR = capacity retention after the respective number of cycles)

CAM	Nb source	Amount	1st DC (base)/mA h g ⁻¹	CR (base)/%	Cycles	Voltage/V vs. Li ⁺ /Li	Ref.
LNO	H ₅ Nb ₃ O ₁₀	1.0 mol%	188.1 (215.9) at 0.1C	91.4 (69.2) at 0.5C	100	2.7–4.3	112
LNO	C ₄ H ₄ NNbO ₉	1.0 mol%	214.1 (233.7) at 0.1C	85.8 (60.1) at 0.5C	200	3.0–4.3	128
LiNi _{0.925} Co _{0.03} Mn _{0.045} O ₂	Nb ₂ O ₅	0.4 mol%	222.7 (219.5) at 0.1C	77.7 (66.3) at 1C	150	2.8–4.3	132
NCM851005	Nb ₂ O ₃	0.3 mol%	210 (210) at 0.1C	97.0 (80.0) at 1C	100	3.0–4.3	152
NCM831106	Nb ₂ O ₅	1.0 mol%	195 (201.8) at 0.1C	86.6 (61.2) at 1C	200	2.8–4.3	120
NCM831106	C ₄ H ₄ NNbO ₉	1.0 mol%	211.8 (195.5) at 0.2C	86.6 (62.6) at 1C	100	2.7–4.4	118
NCM831205 (SC)	Nb ₂ O ₅	1.0 mol%	198.6 (196.8) at 0.1C	92.7 (72.4) at 1C	150	2.7–4.3	129
LiNi _{0.8} Co _{0.2} O ₂	Nb ₂ O ₅	1.0 mol%	190.7 (176.6) at 0.2C	90.0 (58.0) at 5C	100	3.0–4.3	136
LiNi _{0.8} Co _{0.15} Al _{0.05} O ₂	Nb ₂ O ₅	5.0 mol%	192.0 (202.7) at 0.5C	94.2 (69.5) at 0.5C	100	2.8–4.5	133
NMC811	Nb(HC ₂ O ₄) ₅	1.0 mol%	219.6 (203.3) at 0.2C	92.7 (85.3) at 0.2C	100	2.8–4.6	134
NCM811	Nb ₂ O ₅	1.0 mol%	226.3 (213.2) at 0.05C	94.6 (57.6) at 1C	100	2.7–4.3	104
NCM811	Nb ₂ O ₅	0.5 mol%	189.2 (184.9) at 0.1C	91.9 (79.8) at 1C	300	2.75–4.3	119
NCM811	Nb ₂ O ₅	1.0 wt%	202.8 (163.5) at 2C	81 (55) at 2C	200	2.7–4.5	121
NCM811 (SC)	Nb ₂ O ₅	0.5 mol%	226 (202.5) at 0.1C	92.5 (84.3) at 1C	100	2.7–4.3	122
NCM811	Nb ₂ O ₅	1.0 wt%	200.2 (202.3) at 0.1C	90.6 (82.1) at 0.1C	100	3.0–4.3	130
NCM811 (SC)	LiNbO ₃	1.0 mol%	209 (199.2) at 0.2C	91.4 (82.3) at 5C	100	2.7–4.6	123
LiNi _{0.7} Mn _{0.3} O ₂	Nb ₂ O ₅	2.0 mol%	184.3 (185.3) at 0.1C	91.8 (75.8) at 0.2C	50	2.75–4.35	116
NCM712 (SC)	Nb ₂ O ₅	0.05 mol%	204 (200) at 0.1C	85.5 (70.6) at 1C	150	3.0–4.5	145
NCM622	Nb ₂ O ₅	1.0 mol%	188.4 (195.7) at 0.2C	91 (78) at 1C	100	3.0–4.5	78
NCM523	Nb ₂ O ₅	1.0 mol%	159.5 (152.5) at 0.1C	78.7 (73.2) at 0.5C	50	2.5–4.3	131
Li _{1.2} Mn _{0.53} Ni _{0.27} O ₂	Nb(HC ₂ O ₄) ₅	1.6 mol%	248.3 (243.5) at 0.1C	85.5 (57.5) at 1C	200	2.0–4.7	124
Li[Li _{0.2} Ni _{0.2} Mn _{0.6}]O ₂	Nb ₂ O ₅	4.0 mol%	254 (221) at 0.1C	92.3 (83.4) at 0.1C	100	2.0–4.8	117
Li _{1.2} Mn _{0.54} Ni _{0.13} Co _{0.13} O ₂	Nb(HC ₂ O ₄) ₅	2.0 mol%	265.8 (236.3) at 0.2C	86.9 (78.3) at 0.2C	100	2.0–4.8	141
Li _{1.2} Mn _{0.54} Ni _{0.13} Co _{0.13} O ₂	Nb(C ₂ H ₅ O) ₅	3.0 mol%	320 (276) at 0.1C	95 (76) at 0.1C	100	2.0–4.8	137
Li _{1.2} Mn _{0.54} Ni _{0.13} Co _{0.13} O ₂	Nb ₂ O ₅	2.0 mol%	282.6 (265.8) at 0.05C	87.8 (58.5) at 1C	100	2.5–4.6	142

scenarios, the enhanced electrochemical performance can be attributed to the combined effects of doping and coating.¹¹³ Tungsten is a classic example, which almost exclusively migrates to the surface and forms Li_xW_yO_z.¹¹⁴ Indeed, high-valence elements, such as Nb⁵⁺, Ta⁵⁺, W⁶⁺, and Mo⁶⁺, are more likely to have only limited solubility within the crystal structure of Ni-rich CAMs. Specifically, they tend to segregate at the grain boundaries, thereby also suppressing the coarsening of primary particles.^{107,115} This poses an interesting design feature, where known solubility limits can be targeted to create both a bulk and surface modification with a single synthesis procedure. The differentiation between doping and coating can often be ambiguous. In fact, annealing conditions seem to play a pivotal role in material modification. Xin *et al.* reported investigations in this regard, where Nb-based coating and substitution were both observed in Ni-rich CAMs depending on temperature conditions.^{35,59,65,90} Firstly, NCM811 was modified by the hydrolysis process of lithium and niobium ethoxides, a very typical procedure for CAM coatings. With the 500 °C annealing, some Nb⁵⁺ ions were observed to penetrate into the parent material and their concentration maintained around 0.2 at% for a few hundred nanometers. Accordingly, there was a decrease in first-cycle capacity loss, alongside enhancements in rate capability and capacity retention, for half-cells tested in the potential window of 2.8–4.6 V.⁶⁵ Further studies of synchrotron diffraction showed that LiNbO₃ and Li₃NbO₄ phases were initially formed on the CAM surface, and higher temperature treatments (>690 °C) provoked LiNbO₃ decomposition and Nb/TM interdiffusion. In this case, Nb⁵⁺ penetrated into the bulk, resulting consequently in lattice

expansion and cation disordering.^{35,90} Neutron powder diffraction (NPD) analysis suggested higher Ni²⁺ fraction in NCM and interestingly, a manganese replacement in niobium sites of Li₃NbO₄.³⁵ Similarly, several works of Nb-doping of LTMOs also mention the presence of new phases of niobium compounds, particularly when high amounts of dopant are used. The main observed phases in XRD patterns are Li₃NbO₄,^{116–118} LiNbO₃,^{78,104,119} and Nb₂O₅,¹¹⁷ which in general indicates that a solid solution limit was reached and remaining Nb⁵⁺ ions reacted with the available lithium source, as mentioned before for coated CAMs. Therefore, the probable minimal concentration and widespread distribution of these phases in Nb-modified materials hinder their detection with XRD analysis. Nevertheless, either the effect of these new phases is not further considered or the doped materials with higher amount of niobium are not explored due to their low electrochemical performances. In this sense, it is common to encounter a lack of clarity regarding a possible additional coating in Nb-doped CAMs. This is often associated with the use of limited characterization techniques, which may not offer a complete understanding of the modified material. Another source of uncertainty stems from the doping depth, whether Nb⁵⁺ is incorporated into the bulk phase or predominantly resides on the surface. In this context, EDS is commonly utilized, however mostly to solely measure the niobium distribution along the surface. As a matter of fact, considering the studies in which EDS mapping from cross-sectioned particles indicate niobium to be uniformly doped into the bulk phase, there is no agreement in relation to its effect on the material structure.^{104,119–124} Moreover, controlling the exact fraction of



dopant atoms is challenging and can lead to a loss of active species, resulting in inconsistent structural integrity and electrochemical activity. In relation to the surface doping, inhibition of detrimental surface phenomena and facilitated lithium diffusion are achieved, affecting the CAM capacity minimally, combining to a certain extent the advantages of both bulk doping and coating.¹²⁵ Hence, as previously noticed concerning coated materials, a more meticulous analysis involving both the surface and bulk lattice should be considered. It is indeed challenging to precisely describe the interface between coating and doping, and conducting comprehensive studies to assess the effects of different levels of niobium incorporation and gradient characteristics on performance would be complex and demanding.

To illustrate the effects of doping in LTMOs, theoretical studies by means of first-principles simulations have examined niobium as dopant.^{108,126,127} Studies with Ni-rich CAMs revealed that it tends to preferentially occupy the octahedral site in the nickel layer, where exchange energies were the lowest. Chen *et al.* simulated NCM811 doping with high-valence ions (V^{5+} , Nb^{5+} , and Zr^{4+}), and it resulted in a decrease in the quantity of nickel ions in a high valence state.¹⁰⁸ The oxidation states of nickel during delithiation were estimated based on calculated magnetic moments and projected density of states (PDOS). At different lithiation levels, the fraction of Ni^{2+} was slightly higher for the doped NCMs compared to the pristine material. Moreover, at low lithium content, the fractions of Ni^{4+} were lower for the doped samples. From these observations, the authors suggest that high-valence dopants can delay the nickel oxidization, being a promising approach in guiding cathode-redox behavior. Apart from that, M–O binding energies in VO_6 (5.2 eV), NbO_6 (6.2 eV), and ZrO_6 (5.7 eV) were found to be higher compared to that in the NiO_6 octahedron (4.3 eV), indicating that V, Nb, and Zr doping serves as a strategy to suppress oxygen evolution.¹⁰⁸ Yoshida *et al.* reported a theoretical study using 32 candidate elements for optimal co-doping with cobalt in LNO in order to improve cycling performance in LIBs.¹²⁶ Using an optimized framework, a significant and abrupt decrease in the *c*-axis length was observed during the H2 → H3 transition, suggesting that what actually occurred was a “structural change” rather than a “structural transition”. Therefore, a comprehensive screening was performed to identify the optimal doping in LNO able to minimize changes in the *c* parameter. The applied elemental composition ratio was $Ni/Co/X = 0.75 : 0.17 : 0.08$, where within a unit cell, two nickel sites were substituted by cobalt and one nickel site was occupied by X. Fig. 6a and b represents the screening results, with lower values on the vertical axis indicating reduced contractions (see Fig. 6b). For the descriptors of Δd_{ave} , elemental information on the X substitutes (including atomic numbers, atomic radii, *etc.*) was considered. Among all tested doping elements, bismuth and niobium resulted in the smallest contractions. Nevertheless, the energy required for incorporating bismuth into LNO was found to be notably high, implying the limited ability of bismuth to dissolve efficiently within the structure. Consequently, niobium represented the

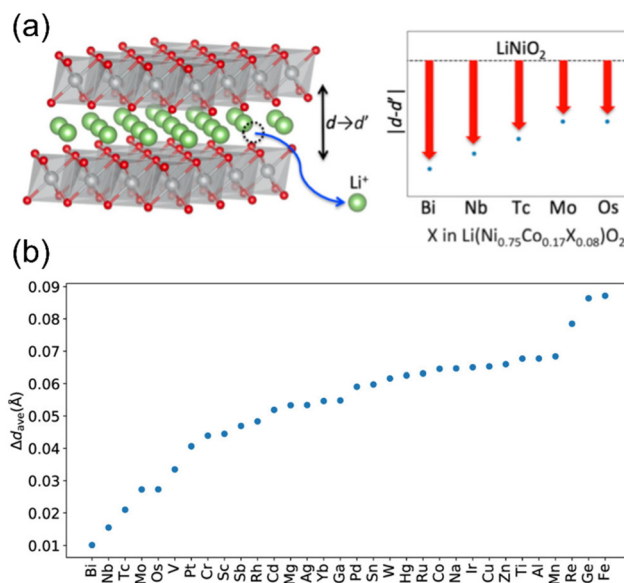


Fig. 6 (a) Representation of layer distance variation as a function of different LNO dopings. (b) Evaluation of *c*-axis contractions induced by 75% charging in terms of Δd_{ave} as a function of doping element. Lower vertical axis values indicate smaller expected contraction and improved cycle performance. Adapted from ref. 126. Copyright 2019, American Chemical Society.

best-known dopant to mitigate interlayer collapse for LNO and likely for LTMOs in general.

Huang *et al.* used a combination of experimental analyses and first-principles calculations to investigate the effect of Nb-doping on the structure and electrochemical properties of LNO.¹¹² Pristine and doped LNO were prepared by a solid-state process using $H_5Nb_3O_{10}$ as Nb-dopant precursor. Accordingly, by XRD analysis, Nb^{5+} (1.0 mol%) was found to be uniformly distributed in the LNO structure, occupying the nickel sites and forming a solid solution. Simulated structures revealed that the Nb-doped LNO exhibits a significantly smaller band gap with lower Fermi level, indicating higher conductivity and improved phase stability, respectively, in comparison to the undoped CAM. Theoretical calculations of the migration energy barrier, along with galvanostatic intermittent titration technique (GITT) experiments, revealed that Nb-doping could effectively enhance the diffusion of Li^+ ions within the material.

In fact, experimental observations for Nb-doping and LTMO structure detail situations, where more in-depth analysis is needed. Starting with examples using LNO, Huang *et al.* reported reduced Ni_{Li}^+ defect fractions based on XRD analysis and lower Ni^{2+} fractions by XPS measurements for the doped material.¹¹² In contrast, Hao *et al.* also reported Nb-doped LNO prepared under same conditions of temperature, in which $Ni(OH)_2$ spheres were coated using a niobium oxide sol (sol-gel method).¹²⁸ In relation to the niobium influence in the CAM structure, its distribution, and effect on electrochemical performance, similar results were obtained. Nevertheless, XRD analysis indicated that Nb-doping causes



stability offered by the Nb-modified LTMO.^{120,122,124,145} Hao *et al.* investigated the electrochemical performance of Nb-doped LNO (1 mol%) at different temperatures (55 to -10 °C), where side reactions at the electrode/electrolyte interface were diminished, especially at higher temperatures, thereby enhancing interfacial stability during cycling.¹²⁸ Apart from that, EIS suggested faster lithium diffusion, even at low temperature. In relation to the material morphology and particle size, no significant changes are generally reported for secondary particles by comparing SEM images before and after doping.^{112,129,130,136,152} On the other hand, when the primary particles are compared, niobium appears to cause a significant reduction in their sizes.^{59,119,120,128,153} Park *et al.* showed an interesting study in this regard using different high-valence elements (Al^{3+} , Nb^{5+} , Ta^{5+} , and Mo^{6+}) to dope LNO.¹¹⁵ The samples were prepared by mixing $\text{Ni}(\text{OH})_2$, LiOH , and dopant precursor, with further calcination within the temperature range of 650 to 800 °C. Changes in primary particle morphology were carefully analyzed by cross-sectional SEM images. While Al-doped LNO displayed similar coarsening behavior to undoped material and maintained its particle shape, primary particles of Nb-, Ta-, and Mo-doped LNO exhibited smaller particle sizes and maintained a radial alignment at each temperature. Fig. 9 displays the cross-sectional images of Nb-LNO compared to LNO. In addition, *in situ* XRD analysis revealed that the dopants formed Li-X-O compounds when introduced to the samples. In the case of Nb-LNO, distinct reflections of LiNbO_3 at temperatures between 450 and 730 °C were identified. At higher temperatures, the peaks gradually weakened and the Li_3NbO_4 phase emerged, remaining stable up to 750 °C. The presence of Li-X-O compounds during high-temperature calcination resulted in grain-boundary coating, inhibiting boundary migration and suppressing primary particle coarsening. Therefore, the mechanism of doping high-valence ions into LNO involved not only bulk incorporation but also grain-boundary coating, affecting the microstructure. The highest discharge capacity was achieved when the cathodes were calcined at 680–700 °C. Ober *et al.* also reported a

similar finding, where the formation of intergranular Li_xNbO_y phases in LNO impeded the growth of its primary particles.¹⁵³ Hence, as previously emphasized, temperature conditions significantly influence niobium modification of LTMOs, and the possibility of an additional coating on the particle surface, including the primary particles themselves, should be considered.

The electrochemical performance of Nb-doped LTMOs shows empirically that there is a significant improvement above the “baseline” material often referenced. Evaluation of cycling (galvanostatic or voltammetric), EIS, and differential capacity analysis are the cornerstone techniques applied and provide much of the basis for the trends observed, however are not the only techniques that should be used, as including physical characterization is very insightful. For example, *operando* XRD studies during the first charge process demonstrated a smooth reversibility of H2 \rightarrow H3 phase transition with a significant suppression of the lattice contraction in Nb-doped samples.^{121–123} Nb-doping (and coating) also seems to inhibit or mitigate oxygen release, as demonstrated by *operando* differential electrochemical mass spectrometry (DEMS).^{123,124,154} *Post-mortem* characterization comprises of easy-to-access SEM, TEM, XRD, and XPS. Microscopy images, in particular from cross sections, serve as an evidence of lower cracking and the better mechanical integrity of doped CAMs.^{59,112,119,121,145} XRD patterns show less lattice distortion and even less $\text{Ni}_{\text{Li}}^{\bullet}$ defects after cycling for the doped sample.¹²⁹ As to the composition of cycled electrodes, XPS exhibited reduced Ni^{2+} formation and lower content of impurities related to the CEI formation or carbonates.^{104,122,129}

Based on our meta-analysis, Nb-doping significantly enhances the performance of LTMOs, as shown in Table 2 and Fig. 7. With regards to capacity, Nb-doping did not have a significant impact with a median relative change of 3.7%. In some reports, the introduction of niobium results in increased values of initial discharge capacity. This enhancement is generally attributed to the diffusion of lithium ions, which is facilitated by the decreased fraction of $\text{Ni}_{\text{Li}}^{\bullet}$ defects and the for-

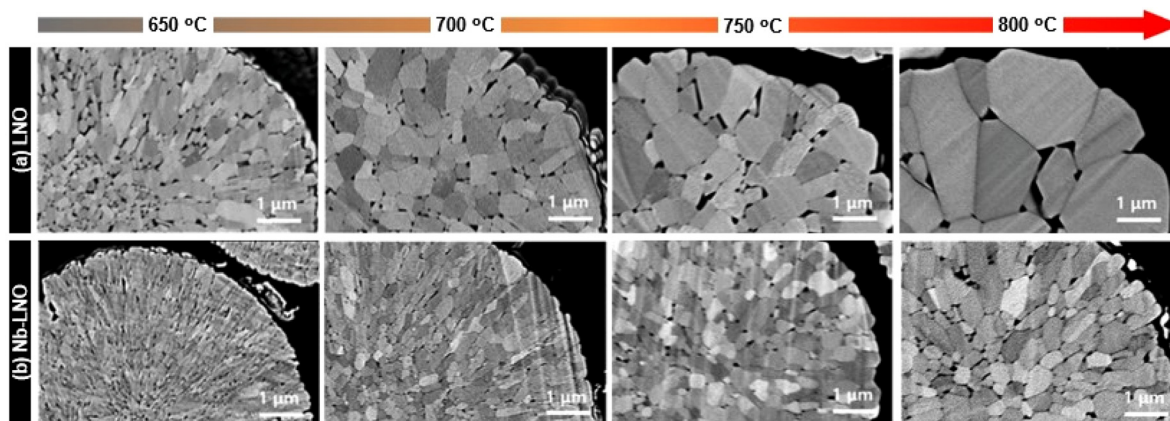


Fig. 9 Cross-sectional SEM images of (a) as-prepared LNO and (b) Nb-LNO calcined at 650–800 °C. Adapted from ref. 115. Copyright 2023, Wiley-VCH GmbH.



- 30 L. Liang, X. Li, M. Su, L. Wang, J. Sun, Y. Liu, L. Hou and C. Yuan, Chemomechanically stable small single-crystal Mo-doped $\text{LiNi}_{0.6}\text{Co}_{0.2}\text{Mn}_{0.2}\text{O}_2$ cathodes for practical 4.5 V-class pouch-type Li-ion batteries, *Angew. Chem., Int. Ed.*, 2023, **62**, e202216155.
- 31 D. Gao, Y. Huang, H. Dong, C. Li and C. Chang, Atomic horizons interpretation on enhancing electrochemical performance of Ni-Rich NCM cathode via W doping: Dual improvements in electronic and ionic conductivities from DFT calculations and experimental confirmation, *Small*, 2023, **19**, 2205122.
- 32 R. Zhang, H. Qiu and Y. Zhang, Enhancing the electrochemical performance of Ni-rich $\text{LiNi}_{0.88}\text{Co}_{0.09}\text{Al}_{0.03}\text{O}_2$ cathodes through tungsten-doping for lithium-ion batteries, *Nanomaterials*, 2022, **12**, 729.
- 33 J. Wang, C. Liu, Q. Wang, G. Xu, C. Miao, M. Xu, C. Wang and W. Xiao, Investigation of W^{6+} -doped in high-nickel $\text{LiNi}_{0.83}\text{Co}_{0.11}\text{Mn}_{0.06}\text{O}_2$ cathode materials for high-performance lithium-ion batteries, *J. Colloid Interface Sci.*, 2022, **628**, 338–349.
- 34 Z. Ahaliabadeh, X. Kong, E. Fedorovskaya and T. Kallio, Extensive comparison of doping and coating strategies for Ni-rich positive electrode materials, *J. Power Sources*, 2022, **540**, 231633.
- 35 F. Xin, H. Zhou, Y. Zong, M. Zuba, Y. Chen, N. A. Chernova, J. Bai, B. Pei, A. Goel, J. Rana, F. Wang, K. An, L. F. J. Piper, G. Zhou and M. S. Whittingham, What is the role of Nb in nickel-rich layered oxide cathodes for lithium-ion batteries?, *ACS Energy Lett.*, 2021, **6**, 1377–1382.
- 36 P. Heitjans, M. Masoud, A. Feldhoff and M. Wilkening, NMR and impedance studies of nanocrystalline and amorphous ion conductors: Lithium niobate as a model system, *Faraday Discuss.*, 2007, **134**, 67–82.
- 37 H. Franke, *Physica status solidi/A*, De Gruyter, 1983, vol. 83, pp. 493–496.
- 38 A. V. Yatsenko, S. V. Yevdokimov and A. A. Yatsenko, Analysis of the ionic contribution to the electrical conductivity of LiNbO_3 crystals, *Ferroelectrics*, 2021, **576**, 157–162.
- 39 Y. Ito and I. Tsuyumoto, Preparation of nanocrystalline LiNbO_3 through aqueous solution process using peroxopoly-niobic acid, *Mater. Chem. Phys.*, 2021, **272**, 125035.
- 40 A. M. Glass, K. Nassau and T. J. Negran, Ionic conductivity of quenched alkali niobate and tantalate glasses, *J. Appl. Phys.*, 1978, **49**, 4808–4811.
- 41 N. Ohta, K. Takada, I. Sakaguchi, L. Zhang, R. Ma, K. Fukuda, M. Osada and T. Sasaki, LiNbO_3 -coated LiCoO_2 as cathode material for all solid-state lithium secondary batteries, *Electrochem. Commun.*, 2007, **9**, 1486–1490.
- 42 G. Hu, Y. Tao, Y. Lu, J. Fan, L. Li, J. Xia, Y. Huang, Z. Zhang, H. Su and Y. Cao, Enhanced electrochemical properties of $\text{LiNi}_{0.8}\text{Co}_{0.1}\text{Mn}_{0.1}\text{O}_2$ cathode materials modified with lithium-ion conductive coating LiNbO_3 , *ChemElectroChem*, 2019, **6**, 4773–4780.
- 43 A. Guéguen, D. Streich, M. He, M. Mendez, F. F. Chesneau, P. Novák and E. J. Berg, Decomposition of LiPF_6 in high energy lithium-ion batteries studied with online electrochemical mass spectrometry, *J. Electrochem. Soc.*, 2016, **163**, A1095–A1100.
- 44 E. Peled, The electrochemical behavior of alkali and alkaline earth metals in nonaqueous battery systems—The solid electrolyte interphase model, *J. Electrochem. Soc.*, 1979, **126**, 2047–2051.
- 45 K. Xu, Interfaces and interphases in batteries, *J. Power Sources*, 2023, **559**, 232652.
- 46 K. Xu, Nonaqueous liquid electrolytes for lithium-based rechargeable batteries, *Chem. Rev.*, 2004, **104**, 4303–4417.
- 47 L. Benitez and J. M. Seminario, Ion diffusivity through the solid electrolyte interphase in lithium-ion batteries, *J. Electrochem. Soc.*, 2017, **164**, E3159–E3170.
- 48 S. Shi, Y. Qi, H. Li and L. G. Hector, Defect thermodynamics and diffusion mechanisms in Li_2CO_3 and implications for the solid electrolyte interphase in Li-ion batteries, *J. Phys. Chem. C*, 2013, **117**, 8579–8593.
- 49 K. Tasaki, A. Goldberg, J.-J. Lian, M. Walker, A. Timmons and S. J. Harris, Solubility of lithium salts formed on the lithium-ion battery negative electrode surface in organic solvents, *J. Electrochem. Soc.*, 2009, **156**, A1019–A1027.
- 50 S.-J. Kwon, S.-E. Lee, J.-H. Lim, J. Choi and J. Kim, Performance and life degradation characteristics analysis of NCM LIB for BESS, *Electronics*, 2018, **7**, 406.
- 51 S. Wenzel, T. Leichtweiss, D. A. Weber, J. Sann, W. G. Zeier and J. Janek, Interfacial reactivity benchmarking of the sodium ion conductors Na_3PS_4 and sodium β -alumina for protected sodium metal anodes and sodium all-solid-state batteries, *ACS Appl. Mater. Interfaces*, 2016, **8**, 28216–28224.
- 52 S. P. Culver, R. Koerver, W. G. Zeier and J. Janek, On the functionality of coatings for cathode active materials in thiophosphate-based all-solid-state batteries, *Adv. Energy Mater.*, 2019, **9**, 1900626.
- 53 J. H. Kim, H. Kim, W. Choi and M. S. Park, Bifunctional surface coating of LiNbO_3 on high-Ni layered cathode materials for lithium-ion batteries, *ACS Appl. Mater. Interfaces*, 2020, **12**, 35098–35104.
- 54 W. Cho, S.-M. Kim, J. H. Song, T. Yim, S.-G. Woo, K.-W. Lee, J.-S. Kim and Y.-J. Kim, Improved electrochemical and thermal properties of nickel rich $\text{LiNi}_{0.6}\text{Co}_{0.2}\text{Mn}_{0.2}\text{O}_2$ cathode materials by SiO_2 coating, *J. Power Sources*, 2015, **282**, 45–50.
- 55 L. Dou, A. Tang, W. Lin, X. Dong, L. Lu, C. Shang, Z. Zhang, Z. Huang, K. Aifantis, P. Hu and D. Xiao, Enhancing the electrochemical performance of $\text{LiNi}_{0.8}\text{Co}_{0.1}\text{Mn}_{0.1}\text{O}_2$ cathodes through amorphous coatings, *Electrochim. Acta*, 2022, **425**, 140745.
- 56 B. Wang, H. Zhao, F. Cai, Z. Liu, G. Yang, X. Qin and K. Świerczek, Surface engineering with ammonium niobium oxalate: A multifunctional strategy to enhance electrochemical performance and thermal stability of Ni-rich cathode materials at 4.5 V cutoff potential, *Electrochim. Acta*, 2022, **403**, 139636.



- 81 X. Liu, J. Shi, B. Zheng, Z. Chen, Y. Su, M. Zhang, C. Xie, M. Su and Y. Yang, Constructing a high-energy and durable single-crystal NCM811 cathode for all-solid-state batteries by a surface engineering strategy, *ACS Appl. Mater. Interfaces*, 2021, **13**, 41669–41679.
- 82 F. Walther, F. Strauss, X. Wu, B. Mogwitz, J. Hertle, J. Sann, M. Rohnke, T. Brezesinski and J. Janek, The working principle of a $\text{Li}_2\text{CO}_3/\text{LiNbO}_3$ coating on NCM for thiophosphate-based all-solid-state batteries, *Chem. Mater.*, 2021, **33**, 2110–2125.
- 83 F. Strauss, S. Payandeh, A. Kondrakov and T. Brezesinski, On the role of surface carbonate species in determining the cycling performance of all-solid-state batteries, *Mater. Futures*, 2022, **1**, 023501.
- 84 A.-Y. Kim, F. Strauss, T. Bartsch, J. H. Teo, J. Janek and T. Brezesinski, Effect of surface carbonates on the cyclability of LiNbO_3 -coated NCM622 in all-solid-state batteries with lithium thiophosphate electrolytes, *Sci. Rep.*, 2021, **11**, 5367.
- 85 M. Nete, W. Purcell, E. Snyders and J. T. Nel, Alternative dissolution methods for analysis of niobium containing samples, *S. Afr. J. Chem.*, 2010, **63**, 130–134.
- 86 W. van den Bergh, H. N. Lokupitiya, N. A. Vest, B. Reid, S. Guldin and M. Stefik, Nanostructure dependence of $\text{T-Nb}_2\text{O}_5$ intercalation pseudocapacitance probed using tunable isomorphic architectures, *Adv. Funct. Mater.*, 2021, **31**, 2007826.
- 87 J. S. Lee and Y. J. Park, Comparison of LiTaO_3 and LiNbO_3 surface layers prepared by post- and precursor-based coating methods for Ni-rich cathodes of all-solid-state batteries, *ACS Appl. Mater. Interfaces*, 2021, **13**, 38333–38345.
- 88 X. Li, L. Jin, D. Song, H. Zhang, X. Shi, Z. Wang, L. Zhang and L. Zhu, LiNbO_3 -coated $\text{LiNi}_{0.8}\text{Co}_{0.1}\text{Mn}_{0.1}\text{O}_2$ cathode with high discharge capacity and rate performance for all-solid-state lithium battery, *J. Energy Chem.*, 2020, **40**, 39–45.
- 89 L. Peng, H. Ren, J. Zhang, S. Chen, C. Yu, X. Miao, Z. Zhang, Z. He, M. Yu, L. Zhang, S. Cheng and J. Xie, LiNbO_3 -coated $\text{LiNi}_{0.7}\text{Co}_{0.1}\text{Mn}_{0.2}\text{O}_2$ and chlorine-rich argyrodite enabling high-performance solid-state batteries under different temperatures, *Energy Storage Mater.*, 2021, **43**, 53–61.
- 90 F. Xin, H. Zhou, J. Bai, F. Wang and M. S. Whittingham, Conditioning the surface and bulk of high-nickel cathodes with a Nb coating: An in situ X-ray study, *J. Phys. Chem. Lett.*, 2021, **12**, 7908–7913.
- 91 R. S. Negi, S. P. Culver, M. Wiche, S. Ahmed, K. Volz and M. T. Elm, Optimized atomic layer deposition of homogeneous, conductive Al_2O_3 coatings for high-nickel NCM containing ready-to-use electrodes, *Phys. Chem. Chem. Phys.*, 2021, **23**, 6725–6737.
- 92 X. Li, J. Liu, M. N. Banis, A. Lushington, R. Li, M. Cai and X. Sun, Atomic layer deposition of solid-state electrolyte coated cathode materials with superior high-voltage cycling behavior for lithium ion battery application, *Energy Environ. Sci.*, 2014, **7**, 768–778.
- 93 G. Lu, W. Peng, Y. Zhang, X. Wang, X. Shi, D. Song, H. Zhang and L. Zhang, Study on the formation, development and coating mechanism of new phases on interface in LiNbO_3 -coated LiCoO_2 , *Electrochim. Acta*, 2021, **368**, 137639.
- 94 H. G. Kim and Y. J. Park, Synergy effect of K doping and Nb oxide coating on $\text{Li}_{1.2}\text{Ni}_{0.13}\text{Co}_{0.13}\text{Mn}_{0.54}\text{O}_2$ cathodes, *J. Electrochem. Sci. Technol.*, 2021, **12**, 377–386.
- 95 L. B. McCusker, R. B. Von Dreele, D. E. Cox, D. Louër and P. Scardi, Rietveld refinement guidelines, *J. Appl. Crystallogr.*, 1999, **32**, 36–50.
- 96 R. Jung, R. Morasch, P. Karayaylali, K. Phillips, F. Maglia, C. Stinner, Y. Shao-Horn and H. A. Gasteiger, Effect of ambient storage on the degradation of Ni-rich positive electrode materials (NMC811) for Li-ion batteries, *J. Electrochem. Soc.*, 2018, **165**, A132–A141.
- 97 Y. Liu, R. Yang, X. Li, W. Yang, Y. Lin, G. Zhang and L. Wang, Nb_2O_5 coating to improve the cyclic stability and voltage decay of Li-rich cathode material for lithium-ion battery, *Molecules*, 2023, **28**, 3890.
- 98 N. Özer and C. M. Lampert, Electrochemical lithium insertion in sol-gel deposited LiNbO_3 films, *Sol. Energy Mater. Sol. Cells*, 1995, **39**, 367–375.
- 99 Y. Deng, C. Eames, J.-N. Chotard, F. Lalère, V. Seznec, S. Emge, O. Pecher, C. P. Grey, C. Masquelier and M. S. Islam, Structural and mechanistic insights into fast lithium-ion conduction in $\text{Li}_4\text{SiO}_4\text{-Li}_3\text{PO}_4$ solid electrolytes, *J. Am. Chem. Soc.*, 2015, **137**, 9136–9145.
- 100 Y. Li, X. Chen, A. Dolocan, Z. Cui, S. Xin, L. Xue, H. Xu, K. Park and J. B. Goodenough, Garnet electrolyte with an ultralow interfacial resistance for Li-metal batteries, *J. Am. Chem. Soc.*, 2018, **140**, 6448–6455.
- 101 L. Chen, K. S. Chen, X. Chen, G. Ramirez, Z. Huang, N. R. Geise, H. G. Steinrück, B. L. Fisher, R. Shahbazian-Yassar, M. F. Toney, M. C. Hersam and J. W. Elam, Novel ALD chemistry enabled low-temperature synthesis of lithium fluoride coatings for durable lithium anodes, *ACS Appl. Mater. Interfaces*, 2018, **10**, 26972–26981.
- 102 S. Breuer, V. Pregartner, S. Lunghammer and H. M. R. Wilkening, Dispersed solid conductors: fast interfacial Li-ion dynamics in nanostructured LiF and $\text{LiF}/\gamma\text{-Al}_2\text{O}_3$ composites, *J. Phys. Chem. C*, 2019, **123**, 5222–5230.
- 103 L. Yang, H. Zhang, J. Chen, H. Chen and Z. Li, Electrical conductivity of Al-doped Li_2ZrO_3 ceramics for Li-ion conductor electrolytes, *Ceram. Int.*, 2021, **47**, 17950–17955.
- 104 J. Li, M. Zhang, D. Zhang, Y. Yan and Z. Li, An effective doping strategy to improve the cyclic stability and rate capability of Ni-rich $\text{LiNi}_{0.8}\text{Co}_{0.1}\text{Mn}_{0.1}\text{O}_2$ cathode, *Chem. Eng. J.*, 2020, **402**, 126195.
- 105 W. Yan, S. Yang, Y. Huang, Y. Yang and G. Yuan, A review on doping/coating of nickel-rich cathode materials for lithium-ion batteries, *J. Alloys Compd.*, 2020, **819**, 153048.
- 106 H. H. Sun, U.-H. Kim, J.-H. Park, S.-W. Park, D.-H. Seo, A. Heller, C. B. Mullins, C. S. Yoon and Y.-K. Sun,



- Transition metal-doped Ni-rich layered cathode materials for durable Li-ion batteries, *Nat. Commun.*, 2021, **12**, 6552.
- 107 G.-T. Park, B. Namkoong, S.-B. Kim, J. Liu, C. S. Yoon and Y.-K. Sun, Introducing high-valence elements into cobalt-free layered cathodes for practical lithium-ion batteries, *Nat. Energy*, 2022, **7**, 946–954.
- 108 Y.-H. Chen, J. Zhang, Y. Li, Y.-F. Zhang, S.-P. Huang, W. Lin and W.-K. Chen, Effects of doping high-valence transition metal (V, Nb and Zr) ions on the structure and electrochemical performance of LIB cathode material $\text{LiNi}_{0.8}\text{Co}_{0.1}\text{Mn}_{0.1}\text{O}_2$, *Phys. Chem. Chem. Phys.*, 2021, **23**, 11528–11537.
- 109 M. F. Kasim, W. A. H. W. Azizan, K. A. Elong, N. Kamarudin, M. K. Yaakob and N. Badar, Enhancing the structural stability and capacity retention of Ni-rich $\text{LiNi}_{0.7}\text{Co}_{0.3}\text{O}_2$ cathode materials via Ti doping for rechargeable Li-ion batteries: Experimental and computational approaches, *J. Alloys Compd.*, 2021, **888**, 161559.
- 110 D. Shumei, T. Dan, L. Ping, L. Huiqin, W. Fenyan and H. Zhang, Research progress and prospect in element doping of lithium-rich layered oxides as cathode materials for lithium-ion batteries, *J. Solid State Electrochem.*, 2023, **27**, 1–23.
- 111 Y. R. Luo, *Comprehensive handbook of chemical bond energies*, CRC Press, 2007.
- 112 G.-X. Huang, R.-H. Wang, X.-Y. Lv, J. Su, Y.-F. Long, Z.-Z. Qin and Y.-X. Wen, Effect of niobium doping on structural stability and electrochemical properties of LiNiO_2 cathode for Li-ion batteries, *J. Electrochem. Soc.*, 2022, **169**, 040533.
- 113 Z. Cui, X. Li, X. Bai, X. Ren and X. Ou, A comprehensive review of foreign-ion doping and recent achievements for nickel-rich cathode materials, *Energy Storage Mater.*, 2023, **57**, 14–43.
- 114 D. Rathore, C. Geng, N. Zaker, I. Hamam, Y. Liu, P. Xiao, G. A. Botton, J. Dahn and C. Yang, Tungsten infused grain boundaries enabling universal performance enhancement of Co-free Ni-rich cathode materials, *J. Electrochem. Soc.*, 2021, **168**, 120514.
- 115 N.-Y. Park, S.-B. Kim, M.-C. Kim, S.-M. Han, D.-H. Kim, M.-S. Kim and Y.-K. Sun, Mechanism of doping with high-valence elements for developing Ni-rich cathode materials, *Adv. Energy Mater.*, 2023, **13**, 2301530.
- 116 Z. Li, C. Luo, C. Wang, G. Jiang, J. Chen, S. Zhong, Q. Zhang and D. Li, Effects of Nb substitution on structure and electrochemical properties of $\text{LiNi}_{0.7}\text{Mn}_{0.3}\text{O}_2$ cathode materials, *J. Solid State Electrochem.*, 2018, **22**, 2811–2820.
- 117 X. Li, H. Xin, Y. Liu, D. Li, X. Yuan and X. Qin, Effect of niobium doping on the microstructure and electrochemical properties of lithium-rich layered $\text{Li}[\text{Li}_{0.2}\text{Ni}_{0.2}\text{Mn}_{0.6}]\text{O}_2$ as cathode materials for lithium ion batteries, *RSC Adv.*, 2015, **5**, 45351–45358.
- 118 T. Li, X. Chang, Y. Xin, Y. Liu and H. Tian, Synergistic strategy using doping and polymeric coating enables high-performance high-nickel layered cathodes for lithium-ion batteries, *J. Phys. Chem. C*, 2023, **127**, 8448–8461.
- 119 F. Tian, Y. Zhang, Z. Liu, R. de Souza Monteiro, R. M. Ribas, P. Gao, Y. Zhu, H. Yu, L. Ben and X. Huang, Investigation of structure and cycling performance of Nb^{5+} doped high-nickel ternary cathode materials, *Solid State Ionics*, 2021, **359**, 115520.
- 120 J. Wang, Z. Yi, C. Liu, M. He, C. Miao, J. Li, G. Xu and W. Xiao, Revealing the effect of Nb^{5+} on the electrochemical performance of nickel-rich layered $\text{LiNi}_{0.83}\text{Co}_{0.11}\text{Mn}_{0.06}\text{O}_2$ oxide cathode for lithium-ion batteries, *J. Colloid Interface Sci.*, 2023, **635**, 295–304.
- 121 M. Chu, Z. Huang, T. Zhang, R. Wang, T. Shao, C. Wang, W. Zhu, L. He, J. Chen, W. Zhao and Y. Xiao, Enhancing the electrochemical performance and structural stability of Ni-rich layered cathode materials via dual-site doping, *ACS Appl. Mater. Interfaces*, 2021, **13**, 19950–19958.
- 122 S. Jamil, M. Fasehullah, B. Jabar, P. Liu, M. K. Aslam, Y. Zhang, S. Bao and M. Xu, Significantly fastened redox kinetics in single crystal layered oxide cathode by gradient doping, *Nano Energy*, 2022, **94**, 106961.
- 123 Z. Zhao, C. Li, Z. Wen, Z. Yang, S. Lu, X. Zhang, S. Chen, B. Wu, F. Wu and D. Mu, Cation mixing effect regulation by niobium for high voltage single-crystalline nickel-rich cathodes, *Chem. Eng. J.*, 2023, **461**, 142093.
- 124 C. Zhang, B. Wei, W. Jiang, M. Wang, W. Hu, C. Liang, T. Wang, L. Chen, R. Zhang, P. Wang and W. Wei, Insights into the enhanced structural and thermal stabilities of Nb-substituted lithium-rich layered oxide cathodes, *ACS Appl. Mater. Interfaces*, 2021, **13**, 45619–45629.
- 125 H. Qian, H. Ren, Y. Zhang, X. He, W. Li, J. Wang, J. Hu, H. Yang, H. M. K. Sari, Y. Chen and X. Li, Surface doping vs. bulk doping of cathode materials for lithium-ion batteries: A review, *Electrochem. Energy Rev.*, 2022, **5**, 2.
- 126 T. Yoshida, K. Hongo and R. Maezono, First-principles study of structural transition in LiNiO_2 and high throughput screening for long life battery, *J. Phys. Chem. C*, 2019, **123**, 14126–14131.
- 127 Y. Liu, X. Wen, R. K. Lake and J. Guo, First-principles study of the doping effect in half delithiated LiNiO_2 cathodes, *ACS Appl. Energy Mater.*, 2023, **6**, 2134–2139.
- 128 Q. Hao, F. Du, T. Xu, Q. Zhou, H. Cao, Z. Fan, C. Mei and J. Zheng, Evaluation of Nb-doping on performance of LiNiO_2 in wide temperature range, *J. Electroanal. Chem.*, 2022, **907**, 116034.
- 129 H. Wu, X. Zhou, C. Yang, D. Xu, Y.-H. Zhu, T. Zhou, S. Xin and Y. You, Concentration-gradient Nb-doping in a single-crystal $\text{LiNi}_{0.83}\text{Co}_{0.12}\text{Mn}_{0.05}\text{O}_2$ cathode for high-rate and long-cycle lithium-ion batteries, *ACS Appl. Mater. Interfaces*, 2023, **15**, 18828–18835.
- 130 Y.-R. Kim, Y.-W. Yoo, D.-Y. Hwang, T.-Y. Shim, C.-Y. Kang, H.-J. Park, H.-S. Kim and S.-H. Lee, Effect of niobium doping to enhance electrochemical performances of $\text{LiNi}_{0.8}\text{Co}_{0.1}\text{Mn}_{0.1}\text{O}_2$ cathode material, *Solid State Ionics*, 2023, **389**, 116108.



- 131 Y. Zhang, C. Cui, J. Liu, Y. Bei, Y. Li, Z. Song, Y. Feng, H. Xu, S. Tian, Y. Song and F. Li, An effective modification strategy enhancing the structure stability and electrochemical performance of $\text{LiNi}_{0.5}\text{Co}_{0.2}\text{Mn}_{0.3}\text{O}_2$ cathode material for lithium-ion batteries, *J. Alloys Compd.*, 2021, **887**, 161480.
- 132 Z. Luo, G. Hu, W. Wang, Z. Peng, Z. Fang, Y. Cao, J. Huang and K. Du, Enhancing structural stability and electrochemical properties of Co-less Ni-rich layer cathode materials by fluorine and niobium co doping, *ACS Appl. Energy Mater.*, 2022, **5**, 10927–10939.
- 133 H. He, J. Dong, D. Zhang and C. Chang, Effect of Nb doping on the behavior of NCA cathode: Enhanced electrochemical performances from improved lattice stability towards 4.5 V application, *Ceram. Int.*, 2020, **46**, 24564–24574.
- 134 Y. Lei, J. Ai, S. Yang, C. Lai and Q. Xu, Nb-doping in $\text{LiNi}_{0.8}\text{Co}_{0.1}\text{Mn}_{0.1}\text{O}_2$ cathode material: Effect on the cycling stability and voltage decay at high rates, *J. Taiwan Inst. Chem. Eng.*, 2019, **97**, 255–263.
- 135 H.-Y. Lee, B.-K. Wu and M.-Y. Chern, Study on the formation of zinc peroxide on zinc oxide with hydrogen peroxide treatment using X-ray photoelectron spectroscopy (XPS), *Electron. Mater. Lett.*, 2014, **10**, 51–55.
- 136 K. Wu, G. Jia, X. Shangguan, G. Yang, Z. Zhu, Z. Peng, Q. Zhuge, F. Li and X. Cui, Improved high rate performance and cycle stability for $\text{LiNi}_{0.8}\text{Co}_{0.2}\text{O}_2$ by doping of the high valence state ion Nb^{5+} into Li^+ sites, *J. Alloys Compd.*, 2018, **765**, 700–709.
- 137 S. Liu, Z. Liu, X. Shen, W. Li, Y. Gao, M. N. Banis, M. Li, K. Chen, L. Zhu, R. Yu, Z. Wang, X. Sun, G. Lu, Q. Kong, X. Bai and L. Chen, Surface doping to enhance structural integrity and performance of Li-rich layered oxide, *Adv. Energy Mater.*, 2018, **8**, 1802105.
- 138 L. Li, E. C. Self, D. Darbar, L. Zou, I. Bhattacharya, D. Wang, J. Nanda and C. Wang, Hidden subsurface reconstruction and its atomic origins in layered oxide cathodes, *Nano Lett.*, 2020, **20**, 2756–2762.
- 139 J. Zhang, Z. Yang, R. Gao, L. Gu, Z. Hu and X. Liu, Suppressing the structure deterioration of Ni-rich $\text{LiNi}_{0.8}\text{Co}_{0.1}\text{Mn}_{0.1}\text{O}_2$ through atom-scale interfacial integration of self-forming hierarchical spinel layer with Ni gradient concentration, *ACS Appl. Mater. Interfaces*, 2017, **9**, 29794–29803.
- 140 E. D. Orlova, A. A. Savina, S. A. Abakumov, A. V. Morozov and A. M. Abakumov, Comprehensive study of $\text{Li}^+/\text{Ni}^{2+}$ disorder in Ni-rich NMCs cathodes for Li-ion batteries, *Symmetry*, 2021, **13**, 1628.
- 141 H. Li, Z. Jian, P. Yang, J. Li, Y. Xing and S. Zhang, Niobium doping of $\text{Li}_{1.2}\text{Mn}_{0.54}\text{Ni}_{0.13}\text{Co}_{0.13}\text{O}_2$ cathode materials with enhanced structural stability and electrochemical performance, *Ceram. Int.*, 2020, **46**, 23773–23779.
- 142 X. Hu, H. Guo, W. Peng, Z. Wang, X. Li and Q. Hu, Effects of Nb doping on the performance of $0.5\text{Li}_2\text{MnO}_3 \cdot 0.5\text{LiNi}_{1/3}\text{Co}_{1/3}\text{Mn}_{1/3}\text{O}_2$ cathode material for lithium-ion batteries, *J. Electroanal. Chem.*, 2018, **822**, 57–65.
- 143 J. Langdon and A. Manthiram, A perspective on single-crystal layered oxide cathodes for lithium-ion batteries, *Energy Storage Mater.*, 2021, **37**, 143–160.
- 144 W. van den Bergh, L. Karger, S. Murugan, J. Janek, A. Kondrakov and T. Brezesinski, Single crystal layered oxide cathodes: The relationship between particle size, rate capability, and stability, *ChemElectroChem*, 2023, **10**, e202300165.
- 145 B. Zhang, L. Cheng, P. Deng, Z. Xiao, L. Ming, Y. Zhao, B. Xu, J. Zhang, B. Wu and X. Ou, Effects of transition metal doping on electrochemical properties of single-crystalline $\text{LiNi}_{0.7}\text{Co}_{0.1}\text{Mn}_{0.2}\text{O}_2$ cathode materials for lithium-ion batteries, *J. Alloys Compd.*, 2021, **872**, 159619.
- 146 V. V. Atuchin, I. E. Kalabin, V. G. Kesler and N. V. Pervukhina, Nb 3d and O 1s core levels and chemical bonding in niobates, *J. Electron Spectrosc. Relat. Phenom.*, 2005, **142**, 129–134.
- 147 D. Norman, X-ray absorption spectroscopy (EXAFS and XANES) at surfaces, *J. Phys. C: Solid State Phys.*, 1986, **19**, 3273–3311.
- 148 B. H. Toby and T. Egami, Accuracy of pair distribution function analysis applied to crystalline and non-crystalline materials, *Acta Crystallogr., Sect. A: Found. Crystallogr.*, 1992, **48**, 336–346.
- 149 P. Kurzahls, F. Riewald, M. Bianchini, H. Sommer, H. A. Gasteiger and J. Janek, The LiNiO_2 cathode active material: A comprehensive study of calcination conditions and their correlation with physicochemical properties. Part I. Structural chemistry, *J. Electrochem. Soc.*, 2021, **168**, 110518.
- 150 D. Goonetilleke, B. Schwarz, H. Li, F. Fauth, E. Suard, S. Mangold, S. Indris, T. Brezesinski, M. Bianchini and D. Weber, Stoichiometry matters: Correlation between antisite defects, microstructure and magnetic behavior in the cathode material $\text{Li}_{1-z}\text{Ni}_{1+z}\text{O}_2$, *J. Mater. Chem. A*, 2023, **11**, 13468–13482.
- 151 A. Chakraborty, S. Kunnikuruvaan, S. Kumar, B. Markovsky, D. Aurbach, M. Dixit and D. T. Major, Layered cathode materials for lithium-ion batteries: Review of computational studies on $\text{LiNi}_{1-x-y}\text{Co}_x\text{Mn}_y\text{O}_2$ and $\text{LiNi}_{1-x-y}\text{Co}_x\text{Al}_y\text{O}_2$, *Chem. Mater.*, 2020, **32**, 915–952.
- 152 Y. Levartovsky, A. Chakraborty, S. Kunnikuruvaan, S. Maiti, J. Grinblat, M. Talianker, D. T. Major and D. Aurbach, Enhancement of structural, electrochemical, and thermal properties of high-energy density Ni-rich $\text{LiNi}_{0.85}\text{Co}_{0.1}\text{Mn}_{0.05}\text{O}_2$ cathode materials for Li-ion batteries by niobium doping, *ACS Appl. Mater. Interfaces*, 2021, **13**, 34145–34156.
- 153 S. Ober, A. Mesnier and A. Manthiram, Surface stabilization of cobalt-free LiNiO_2 with niobium for lithium-ion batteries, *ACS Appl. Mater. Interfaces*, 2023, **15**, 1442–1451.
- 154 F. Strauss, D. Kitsche, Y. Ma, J. H. Teo, D. Goonetilleke, J. Janek, M. Bianchini and T. Brezesinski, Operando characterization techniques for all-solid-state lithium-ion batteries, *Adv. Energy Sustainability Res.*, 2021, **2**, 2100004.

